

On the Dynamics of ECL Inverter based Ring Oscillators

Sandeepa Sarkar
Burdwan Harisava Hindu Girls' High School (Morn)
Burdwan, India
e-mail: sandeepaphys@gmail.com

Bishnu Charan Sarkar
Dept. of Physics
The University of Burdwan
Burdwan, India
e-mail: bcsarkar_phy@yahoo.co.in

***Abstract*—**The effect of electrical variations in free running frequency and in the dynamics of BJT based Ring Oscillator (RO) have been thoroughly examined in this paper. Techniques of electronic frequency tuning of an emitter coupled inverter based RO have been experimentally studied. The oscillation frequency of the RO depends on the dc reference voltage and the dc bias current. An analytical explanation of the observed results has been incorporated in this paper. The dynamics of the said hardware experimental circuit also have been scrupulously examined. It is observed that a periodic oscillation starts for a given reference voltage and gradual variations of the reference voltage in this region give rise to different multi periodic and chaotic oscillations. A higher order nonlinear mathematical model of the RO circuit has been proposed and the system has been numerically studied. The numerical simulations results support the experimental observations.

Keywords-*Electrical tuning; Ring Oscillator; Chaotic Ring Oscillator; Nonlinear mathematical model of Ring Oscillator.*

*****

I. INTRODUCTION

Ring Oscillators (ROs) are versatile building blocks of several electronic systems such as coherent communication receivers, frequency synthesizers, multiphase clock signal generators etc. [1-5]. In spite of the less spectral purity of output signal of RO, other various properties like the satisfactory speed of operation, noise performance, simplicity of design, possibility of easy IC realization of the system etc. have made the RO an attractive signal generator. During last few decades, a large number of researches have been done on generation of wave form, control of frequency and speed of operation, minimization of phase noise etc. in RO. A survey of recent literature reveals that, besides periodic oscillation, RO can be brought into chaotic oscillatory region by using some suitable technics [6-7]. But, to the knowledge of the authors, generation of chaos in a simple 3-stage inverter based RO by varying only some circuit parameter has not been thoroughly investigated. Chaotic signals have a few unique characterizing properties which have made it attractive in communication applications [8-9]. It is predicted that voltage tuned ROs have rich application potential in chaos based communication systems, where representation of information bits as chaotic signals is an important design requirement. For this purpose, an electrical control of some design parameters of chaos generator circuits would obviously be of importance. In this work, we model a practical three stage Emitter Coupled Inverter (ECI) based RO. And we also propose a nonlinear mathematical model of this type of RO circuit.

The paper has been organized in the following way. The details of hardware experimental arrangement of three stage ECL (Emitter Coupled Logic) inverter based RO along with the obtained results are given in section II. The frequency of oscillation of the RO has been observed to depend on the value of the dc reference voltage and the dc bias current of the inverter stages. It has also been observed that the RO shows different complex behaviors like period doubling and chaos for certain range of values of reference voltage control parameters. Section III describes a semi analytical explanation of the tuning properties of the ECI based RO. Developing a suitable nonlinear mathematical model of emitter coupled inverter, system equations of RO circuit are formulated in section IV. A linear analysis of system equations is described in section V. It contributes indications of the values of system parameters necessary for the transition from a stable non-oscillatory to an unstable oscillatory state. In section VI, system equations are studied through numerical simulation. Numerically simulated results are in good agreement with the experimental observations. Finally, some concluding remarks have been included in section VII.

II. ECL INVERTER BASED RO

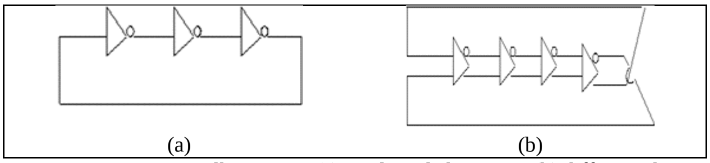

Figure 1. Ring oscillator using (a) single ended inverter, (b) differential inverter.

RO is simply a chain of inverter-stages associated in cascade and in a closed loop as shown in Fig. 1. The steady oscillation in a RO requires a unity closed loop gain and a total phase shift of 2π respectively. In the literature one can find several techniques of inverter implementation [10-12]. In our present work we have used ECL OR-NOR logic inverters to construct RO, because of some advantages of it. ECL logic is non-saturated logic. Moreover, complementary outputs can be achieved which makes the designed procedure of the oscillator simple. The technique we have used here to construct the RO is that we connect the inverting output of one stage to the next stage and the output of the last stage is feedback to the first. Here odd numbers of gates (at least 3 stages) are necessary to satisfy the condition of sustained oscillation and each stage is driven by a suitable reference voltage. The block diagram of such 3-stage RO is shown in Fig. 2.

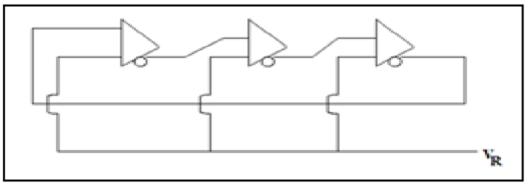

Figure 2. Functional block diagram of the 3-stage inverter based RO.

ISSN: 2454-4248
424 – 431

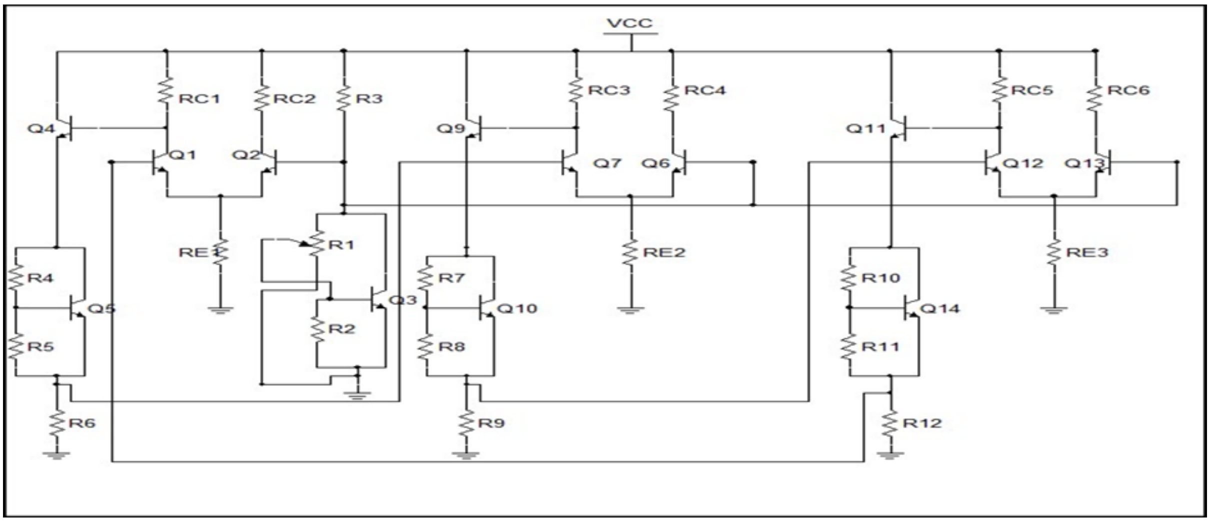

Figure 3. Circuit diagram of ECI based 3-stage Ring Oscillator. The values of circuit components: RC1 to RC6 = 1KΩ, RE1 to RE3 =1.4KΩ, R6=R9 = R12=1KΩ. All the other resistors =10KΩ. R1 is a variable resistor. Reference voltage is changed by varying the resistance R1. The transistors used in the circuit belong to transistor array CA3086; DC supply voltage Vcc = 5.2 volts.

A. Experimental Studies of 3-Stage RO

A RO has been designed using three ECIs. The hardware arrangement of the experimental setup is shown in Fig. 3. All the bipolar junction transistors used in the experimental circuit belong to IC chips namely CA3086 which is a transistor array. The basic inverter circuit contains two emitter coupled BJTs, two load resistors, RCs, a V_{BE} multiplier type voltage reference circuit. Here, two consecutive inverters are connected through a buffer and a dc level shifter. These have been realized using an emitter follower amplifier (as a buffer) along with a V_{BE} multiplier (for dc level shifting).The required reference voltage of an ECI is taken from the V_{BE} multiplier type voltage reference circuit. Once adjusted, this circuit provides a stable reference voltage in the face of any unwanted changes in the dc supply voltage or in the ambient temperature. We have performed our hardware experimental study in two fold way.

a) electrical tuning of frequency of oscillation

In the first phase of our experiment, the dependence of oscillation frequency (f_0) on the dc reference voltage (V_R) and the dc bias current (I_Q) has been studied. The value of V_R has been varied by changing the resistance used in the V_{BE} multiplier circuit and for each value of V_R corresponding f_0 has been measured. Fig. 4(a) shows variation of f_0 with V_R for three different values of dc bias current, I_Q. It has been observed that f_0 decreases with the increase of V_R.

A 'current mirror' type biasing circuit has been designed for the variation of the dc bias current in the inverter amplifier [13]. It has been observed that by changing the value of the variable resistor in the current mirror circuit, the bias current can be controlled. For different values of the bias current (I_Q), free running frequency, f_0 of the RO has been measured. The obtained results are shown graphically in Fig 4(b) that indicates f_0 decreases as I_Q increases.

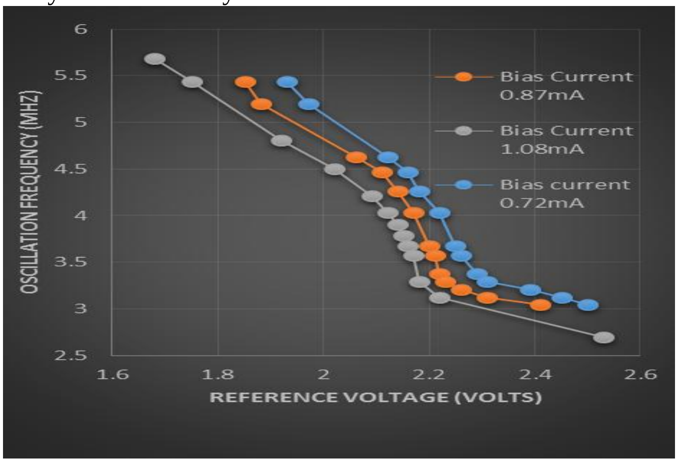

(a)

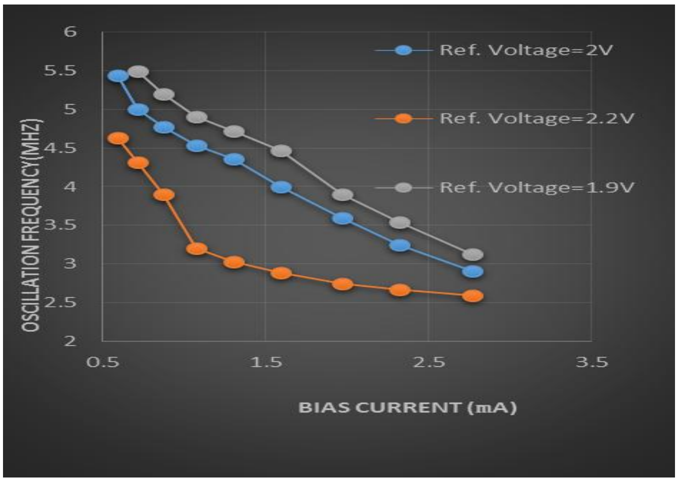

(b)

Figure 4. Experimentally obtained variation of frequency of oscillation of three-stage Ring Oscillator with (a) increase of reference voltage, VR (b) increase of bias current, IQ.

ISSN: 2454-4248
424 – 431

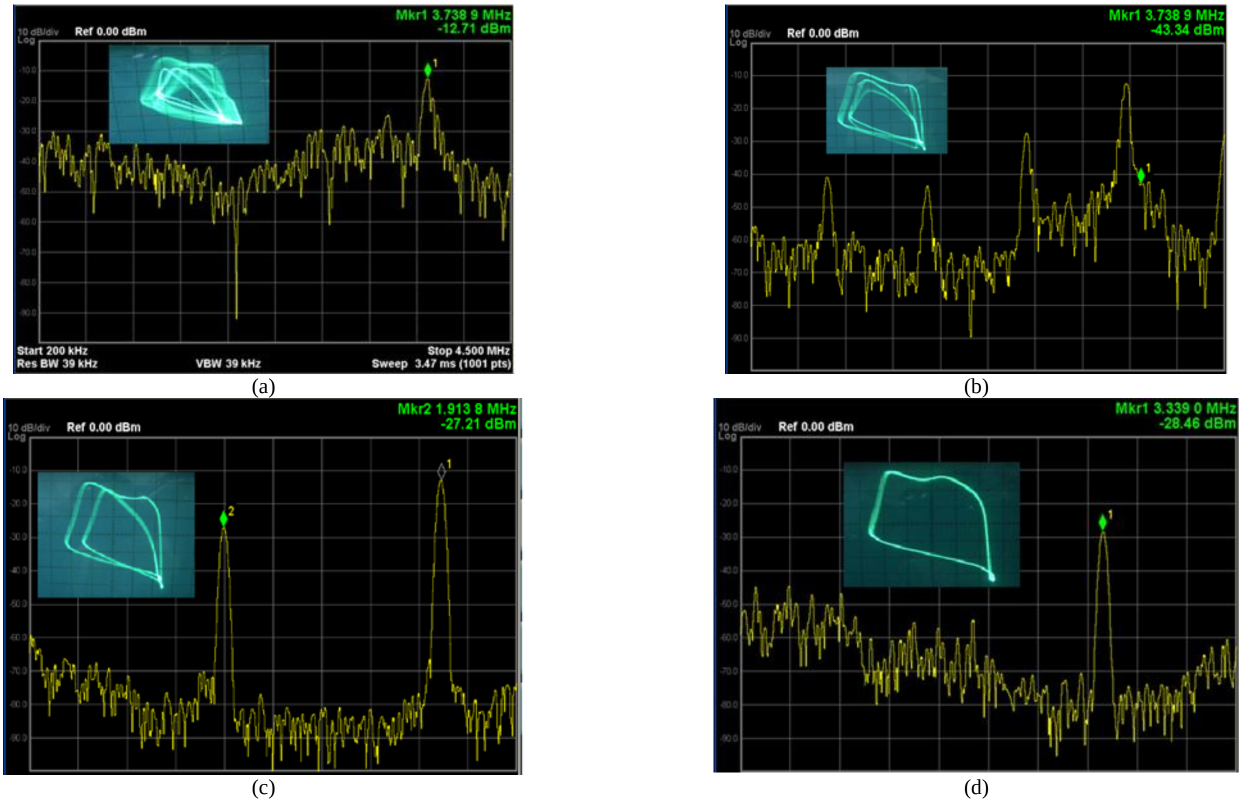

Figure 5. Experimentally obtained output spectra and phase plane plot (inset) of RO for different values of Reference voltage VR, (a) VR =1.5V, (b) VR =1.55V, (c) VR =1.65V, (d) VR=1.7V.

b)Aappearance of complex dynamics

In the second phase of our experimental study some interesting phenomenon has been observed when we minutely investigate the building up of oscillation. As we very slowly increase V_R from zero, no oscillation is observed at RO output until V_R <1.49 volts. As V_R has just crossed this limit, instead of stable oscillating state, several complicated states are observed. At V_R = 1.49volts chaotic attracters are observed at RO output. As V_R increases, chaotic oscillations of RO remains up to V_R =1.55volts. When V_R becomes greater than 1.55volts, chaotic oscillation transit to period-4 and with further increase in V_R, period-2 (V_R=1.65volts) and then periodic oscillations building up. However, it is detected that, while V_R is slowly increased form zero, before the system has reached into the stable oscillating state, it passes through several complicated states such as broad band continuous spectra, multiple discrete components etc. These states are equivalent to well-known chaotic state and quasi-periodic state of oscillation. In the decreasing condition of the bias voltage, the oscillator transits from the stable oscillating state to no oscillating state through multi-periodic and chaotic states again. These observations are obtained from the time development of the oscillator output voltage, the state space trajectories between the voltages taken from the output points of two consecutive inverters and the spectral characteristics of the oscillator outputs. Fig. 5(a) to 5(d) show the output spectra and phase plane plots (inset) of outputs taken from two different points of the ring oscillator in the increasing mode for four different values of V_R. They specify different dynamical states (chaotic, multi periodic and periodic) of the oscillator.

III. SEMI ANALYTICAL EXPLANATION OF TUNING PROPERTIES

It is possible to explain qualitatively the behavior of frequency tuning of RO without formulating the exact system equations. To describe the frequency tuning characteristics of an ECL inverter based RO, we have to study the principle of operation of a single inverter stage.

A. Operating principle of a single inverter stage

Fig. 6 shows the circuit diagram of a single inverter stage. Here emitters of two transistors are coupled together. These two transistors are switched in between cutoff and active mode. If the collector currents of transistors Q1 and Q2 be I_{c1} and I_{c2} respectively, then from the transistor current equation one can write:

$$I_{c1} = I_{01}\exp\left(V_{BE1}/V_T\right) \quad , \qquad (1.1)$$

$$I_{c2} = I_{02}\exp\left(V_{BE2}/V_T\right). \qquad (1.2)$$

Where, V_T (= ηKT/e, K is Boltzmann constant, e is the electronic charge, T is the absolute temperature of the junction, η is the dimensionless number depending on the semiconductor) is called the voltage equivalent of temperature. At room temperature (300K), V_T = 26mV. And I_{01} and I_{02} are the reverse saturation currents of the two transistors respectively. $V_{BE1} = (V_i – V_e)$, $V_{BE2} = (V_R – V_e)$. Wher V_e is the voltage across the coupled emitter terminal. Since Q1 and

 ISSN: 2454-4248
424 – 431

Q2 are two identical transistor, then, $I_{01} = I_{02}$ and $I_{c1}/I_{c2} = \exp\{(V_{BE1} - V_{BE2})/V_T\} = \exp\{(V_i - V_R)/V_T\}$.

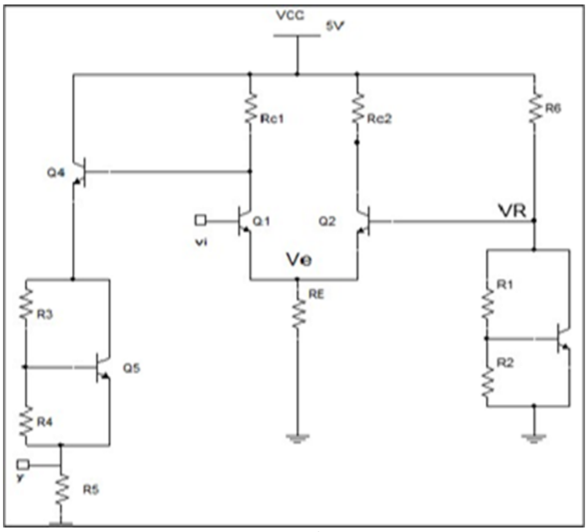

Figure 6. Experimental Circuit of Single ECL Inverter stage.

The two output voltages V_{01} and V_{02} will be

$V_{01} = V_{CC} - Rc1I_{c1}$, (2.1)

$V_{02} = V_{CC} - R_{c2}I_{c2}$. (2.2)

When voltage equivalent of temperature (V_T) is very low in comparison with voltage difference between two inputs V_i and V_R, $\{V_T < (V_i - V_R)\}$, then, $I_{c1} >> I_{c2}$ and practically transistor Q1 is conducting and Q2 remains OFF. So the value of V_{01} is low ($V_{CC} - R_{c1}I_{c1}$) and V_{02} is high (V_{CC}). This implies that if $V_i > V_R$, then V_{01} is low ($V_{CC} - R_{c1}I_{c1}$) and V_{02} is high (V_{CC}).Similarly, if $V_i < V_R$, then $V_{01}$is high (V_{CC}) and V_{02} is low ($V_{CC} - R_{c2}I_{c2}$). Therefore we can conclude that V_{01} is the inverting output and V_{02} is the non-inverting one. It is needless to mention, only the inverting output is required in our present work. The shifting of output level is necessary in order to maintain the convention of high and low state across V_R. Here it is done with the help of V_{BE} multiplier. In this context the shifting should be such that the high output must lie 0.5 volts above the reference voltage level and low output must lie 0.5 volts below the reference level, V_R.

B. Qualitative explanation of frequency variation

It is already declared that the values high (V_{OH}) and low (V_{OL}) levels of inverting output is

$V_{OH} = V_{CC}$, (3.1)

$V_{OL} = V_{CC} - R_cI_c$. (3.2)

Here I_c and R_c is the collector current of the inverting transistor. Thus the two levels of buffer amplifier output V_{BH} and V_{BL} are given as

$V_{BH} = V_{OH} - \Delta V_x$, (4.1)

$V_{BL} = V_{OH} - \Delta V_x - R_cI_c$. (4.2)

ΔV_x is the amount of voltage level shift due to the buffer amplifier and the level shifting circuit. These values are to be adjusted knowing the value of reference voltage, V_R. The output of buffer amplifier is adjusted as either more than V_R by an amount ΔV_1 or less than V_R by an amount ΔV_2. So,

$V_{BH} = V_R + \Delta V_1$ (5.1)

$V_{BL} = V_R - \Delta V_2$ (5.2)

Hence for a particular value of reference voltage V_R, one gets the value of ΔV_1 and ΔV_2 as,

$\Delta V_1 = V_{CC} - \Delta V_x - V_R$ (6.1)

$\Delta V_2 = V_R - (V_{CC} - \Delta V_x - R_cI_c)$ (6.2)

So for the conduction of the transistor of the inverter, its input voltage must be increased more than ΔV_2. This change occurs by the changing of the input capacitance of the transistor by a current obtained from the previous buffer amplifier. Considering the charging current to be fixed, we note that the time required for the change of the input voltage by the said amount depends on two quantities chosen by the designer: the reference voltage and the bias current. Thus the inherent time delay in the chain of inverters can be altered by the change of these two quantities. This would in turn change the frequency of RO. Further, in both the cases either with the increase of V_R or increase of Ic, charging voltage increases and more time is required to attain this voltage. Due to this reason propagation delay of each stage of the RO increases which results in decrease of the frequency of oscillation (f_0). Therefore, experimental observations as presented in Fig. 4(a) and Fig. 4(b) can be explained qualitatively according to this concept.

IV. NONLINEAR MODEL OF THREE STAGE ECL INVERTER BASED RO

To get a complete comprehension of the observed complexity and chaotic behaviors of the ring oscillator circuit under study, apart from experimental observation details theoretical analysis is also crucial. For this, mathematical modeling in the replacement of the actual hardware circuit also has been included here. As mentioned earlier and in [7], basic principle of RO is based on the charging and discharging of a capacitor C_P connecting between the input and output of an inverter. This capacitor arises from obvious parasitic in the internal structure of the inverter. For the BJT, it is the combination of junction capacitances C_{be} and C_{bc}. Fig.7 shows the symbol of an inverter with a capacitor, C_P linked between the inverter's input and output. At low frequencies, this capacitor has a very high impedance and V_i is phase inverted. At very high frequencies it behaves like short circuit and hence V_i can no longer be inverted; i.e., V_i and V_0 are in phase. Therefore there exists a bandwidth within which the inverter properly introduces the required phase inversion. We have taken higher-order nonlinear models of three-stage RO based on ECL inverter.

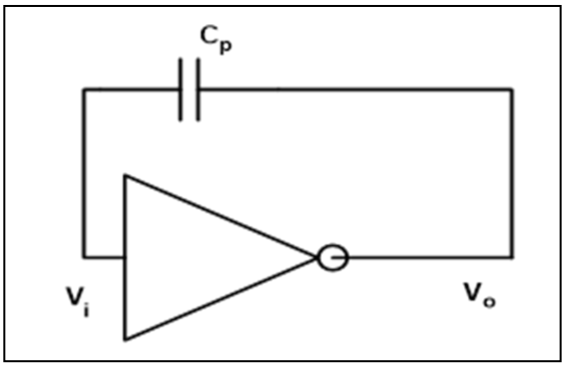

Figure 7. Digital inverter symbol with parasitic capacitor C_P.

ISSN: 2454-4248
424 – 431

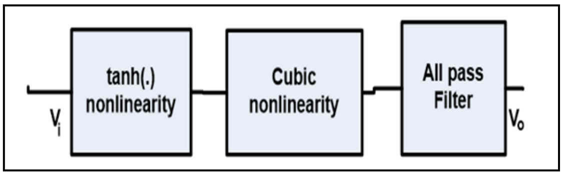

Figure 8. Proposed nonlinear model of single emitter coupled inverter stage.

Proposed model of inverter is composed of a tanh(.) nonlinear stage, an all pass filter stage and an additional cubic type nonlinear stage(shown in Fig. 8). As mentioned in [7] the choice of the tanh(.) nonlinearity is inspired by the fact that the relation between the input and output differential voltages of a bipolar transistor differential pair is $V_0 = -V_{sat}\tanh(V_i/V_s)$, V_{sat} is a saturation voltage and V_s is used to adjust the internal slope; i.e., how sharp is the transition from V_{sat} to $-V_{sat}$. The all-pass filter (transfer function is $T(s) = (1-T_s)/(1+T_s)$) represents the effect of C_P where, $T=C_P.r_{out}$ is the filter time constant and r_{out} is the output resistance of the inverter. Cubic nonlinearity originates from the typical nonlinearity of the transistor which is used to maintain the reference voltage level of inverter operation. Cubic type dynamical dependence of current and voltage in a BJT based circuit is very common. In our working circuit, an inverter's input is practically the difference between real time input voltage and the reference voltage, V_R. V_R is supplied from a voltage divider circuit whose active component is a BJT. To investigate the existence of nonlinear dependence of output on differential input, we measure the variation of V_0 with that of $(V_R - V_i)$ in a bipolar transistor based experimental circuit using PSPICE software which is depicted in Fig. 9.

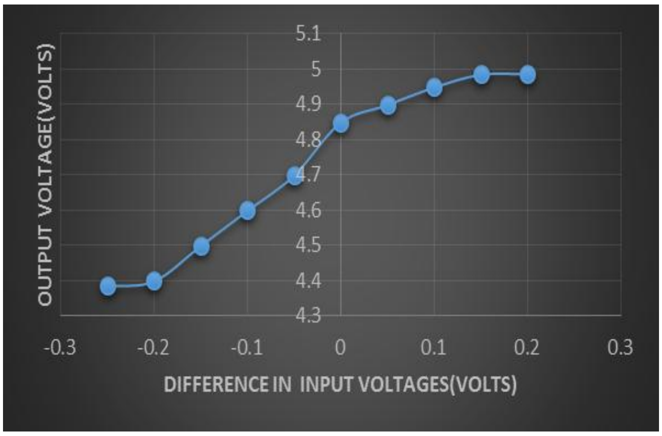

Figure 9. Variation of ECI output (V_0) with its effective input (V_R - V_i).

The mathematical relation between output voltage and effective input voltage of a differential inverter now can be established from the nature of the experimentally obtained curve. From the voltage transfer characteristics curve, we choose an additional nonlinearity along with tanh(.) one as power of V_i having linear and cubic terms with suitable weight parameters. The quadratic term is not taken to ensure the odd symmetric nature of V_0 as a function of V_i. By proper choice of these aforesaid parameters, we write the relation of V_0 as

$V_0 = -V_{sat}\tanh[(aV_i - bV_i^3)/V_s]$, here a and b are reference voltage dependent parameters. Naturally magnitude of b is much less than that of a, since the response is linear for small values of V_i.

Therefore the behavior of an inverter represents by the differential equation given bellow:-

$$V_0+TV_0' = -V_{sat}.\tanh[(aV_i - bV_i^3)/V_s] + T(V_{sat}/V_s)[1 - \tanh^2[(aV_i - bV_i^3)/V_s]]\,V_i'. \quad (7)$$

Dimensionless form of the above equation will be

$$y+y' = -\beta\tanh(\alpha(ax - bx^3)) + \beta\alpha[1 - (\tanh^2(\alpha(ax - bx^3))]x. \quad (8)$$

We have introduced the dimensionless variables $x= V_i/V_{ref,}$, $y= V_0/V_{ref,}$, $\alpha=V_{ref}/V_s$, $\beta=V_{sat}/V_{ref}$, time is normalized with respect to T and V_{ref} is an arbitrary reference voltage. $A\beta= V_{sat}/V_{s} \rightarrow$the internal gain of the amplifier.

A. Formulation of system equations

To formulate the overall system equations we have to consider such three stages cascaded in a loop and each stage is represented by equation similar as (8). Considering such three stages in a closed loop, the overall system is described by:-

$$x' = -x - \beta\tanh(\alpha(az - bz^3)) + \beta\alpha[1 - (\tanh^2(\alpha(az - bz^3))]z', \quad (9.1)$$
$$y' = -y - \beta\tanh(\alpha(ax - bx^3)) + \beta\alpha[1 - (\tanh^2(\alpha(ax - bx^3))]x', \quad (9.2)$$
$$z' = -z - \beta\tanh(\alpha(ay - by^3)) + \beta\alpha[1 - (\tanh^2(\alpha(ay - by^3))]y'. \quad (9.3)$$

Where x,y,z are the normalized outputs of the three inverters. Prime (′) over the variables represents derivative with respect to normalized time T. In order to derive a condition for oscillation, we have to linearize the above system.

V. STABILITY OF THE EQUILIBRIUM POINTS OF THE SYSTEM WITH THE VARIATION OF REFERENCE VOLTAGE

In the analytical study of RO dynamics, first we evaluate the equilibrium points (X*,Y*,Z*) in the three dimensional state space by equating the time derivatives of the state variables x,y, z to zero in equation (9). This gives three possible equilibrium points:(0,0,0),$\{((1+A^3a^3)/A^3a^2b(1+A^2a^2+A^4a^4))^{0.5}, ((1+A^3a^3)/A^3a^2b(1+A^2a^2+A^4a^4))^{0.5}, ((1+A^3a^3)/A^3a^2b(1+A^2a^2+A^4a^4))^{0.5}\}$ and $\{-((1+A^3a^3)/A^3a^2b(1+A^2a^2+A^4a^4))^{0.5}, -((1+A^3a^3)/A^3a^2b(1+A^2a^2+A^4a^4))^{0.5}, -((1+A^3a^3)/A^3a^2b(1+A^2a^2+A^4a^4))^{0.5}\}$. Where $A = \alpha.\beta$ is the loop gain.

In order to derive a condition for oscillation, we do an approximation of the above system equations in (9) and separate variables to obtain the equations in (10).

Next we formulate the Jacobean matrix of the system described by (10) at respective equilibrium points and derive the Eigen values of the characteristic equation. The characteristic equation is written as $\det(J - \boldsymbol{\lambda}I) = 0$, I is the identity matrix and $\boldsymbol{\lambda}$ is the Eigen value of Jacobian matrix. So for the system under study we get characteristics equation in the form as shown in (11).

ISSN: 2454-4248
424 – 431

$$x^{\cdot} = \frac{1+A^3a}{A^3-1}x - \frac{A^3b}{A^3-1}x^3 + \frac{A^2(1+a)}{A^3-1}y - \frac{A^2b}{A^3-1}y^3 + \frac{A(1+a)}{A^3-1}z - \frac{Ab}{A^3-1}z^3 \quad (10.1)$$

$$y^{\cdot} = \frac{A(1+a)}{A^3-1}x - \frac{Ab}{A^3-1}x^3 + \frac{1+A^3a}{A^3-1}y - \frac{A^3b}{A^3-1}y^3 + \frac{A^2(1+a)}{A^3-1}z - \frac{A^2b}{A^3-1}z^3 \quad (10.2)$$

$$z^{\cdot} = \frac{A^2(1+a)}{A^3-1}x - \frac{A^2b}{A^3-1}x^3 + \frac{A(1+a)}{A^3-1}y - \frac{Ab}{A^3-1}y^3 + \frac{1+A^3a}{A^3-1}z - \frac{A^3b}{A^3-1}z^3 \quad (10.3)$$

$$\begin{pmatrix} \frac{(1+A^3a)-3A^3bx^{*2}}{(A^3-1)} - \lambda & \frac{A^2(1+a)-3A^2by^{*2}}{(A^3-1)} & \frac{A(1+a)-3Abz^{*2}}{(A^3-1)} \\ \frac{A(1+a)-3Abx^{*2}}{(A^3-1)} & \frac{(1+A^3a)-3A^3by^{*2}}{(A^3-1)} - \lambda & \frac{A^2(1+a)-3A^2bz^{*2}}{(A^3-1)} \\ \frac{A^2(1+a)-3A^2bx^{*2}}{(A^3-1)} & \frac{A(1+a)-3Aby^{*2}}{(A^3-1)} & \frac{(1+A^3a)-3A^3bz^{*2}}{(A^3-1)} - \lambda \end{pmatrix} = 0 \quad (11)$$

Here x^*,y^*,z^* indicate the value of x, y and z respectively at a particular equilibrium point. Expanding (11) we obtain

$$P_3\boldsymbol{\lambda}^3+P_2\boldsymbol{\lambda}^2+P_1\boldsymbol{\lambda}+P_0 = 0 \quad (12)$$

Here, the coefficients P_0, P_1, P_2, P_3 will depend on the values of system parameters and the location of fixed point considered. The nature of the roots of the characteristic equation is obtained by applying the Routh-Hurwitz's criteria [14], and hence the stability of a particular equilibrium point can be predicted. The equilibrium point would be stable if the roots of (12) have negative real parts. According to Routh- Hurwitz's criteria, this is possible if,

$P_0>0$ (13.1)
$P_1>0$ (13.2)
$P_1P_2-P_0P_3>0$ (13.3)

Among the equilibrium points mentioned above origin (0, 0, 0) is a trivial point because it does not satisfy (13.3).
The values of coefficients are

$P_3 = 1$ (14.1)

$P_2=3(3A^3bX^{*2}-(1+A^3a))/(A3-1)$ (14.2)

$P_1=[3((1+A^3a)-3A^3bX^{*2})^2-2(A^2(1+a)-3A^2bX^{*2})(A(1+a)-3AbX^{*2})]/(A^3-1)^2$ (14.3)

$P_0=[3(A(1+a)-3AbX^{*2})(A^2(1+a)-3A^2bX^{*2})(1+A^3a-3A^3bX^{*2})-(1+A^3a-3A^3bX^{*2})^3-(A^2(1+a)-3A^2bX^{*2})^3-(A(1+a)-3AbX^{*2})^3]/(A^3-1)^3$ (14.4)

We put $x^*= y^*= z^*= X^*$, because they all have same values for a specific equilibrium point.

Then to get a stable state of the system, P_2 should be greater than zero. Varying the magnitude of a one can change the value of P_2 from positive to negative through zero keeping the loop gain A unaltered. Thus the system would become unstable from a stable condition by the variation of a (i.e. the reference voltage). The critical value of a (a_c) is obtained by equating P_2 to zero. It gives,

$$A^7a_c^{\,7}+A^4a^{c6}+A^5a_c^{\,5}+A^2a_c^{\,4}-2A^3a_c^{\,3}+a_c^{\,2}=3 \quad (15)$$

At $a = a_c$, the real parts of the pair of complex roots of (10) become zero (from negative value) leading to limit cycle of oscillation of the system. This is well known Hopf bifurcation of the nonlinear system. .However, the complete picture of the CO dynamics can be understood from the detailed nonlinear analysis of the system equations.

VI. Numerical analysis

To realize the complete effect of reference voltage one has to analyze system equations in (9) without any linear approximations. The numerical solution of these equations for a carefully chosen set of system parameters can throw much light into the dynamics of the system. For this purpose the set of (9) has been solved using 4th order Runge-Kutta algorithm in the normalized time domain [15]. A small value of the time step (h) also leads this process towards a very good integration result. We have used a very small value of time step h = 0.01 for the simulation done here. To obtain steady state values of the state variables, a good number of values close to t =0 have been discarded for rejection of initial transients. The values of different parameters have been chosen taking the elements of the experimental hardware circuit into consideration (described in section 2). It is observed that for a < 0.5, the state variables are fixed at (0, 0, 0), indicating a stable equilibrium state. At a =0.7 the obtained time development of the state variable x has become unstable and a chaotic oscillation is observed. Fig. 10(a) to Fig. 10(d) depict respectively the numerically obtained results for different reference voltages. They provide the state- space trajectories in x - y plane. With gradual increase in the value of a, chaotic regime shift into multi- period cycles and finally a stable limit cycle is observed. This is evident from the results shown in Fig. 10(b) (Period-4), Fig. 10(c) (Period-2) and Fig. 10(d) (periodic) respectively.

To obtain a complete picture of the RO behavior with the change in reference voltage, a one dimensional bifurcation diagram of the oscillator output with a as control parameter is drawn.

 ISSN: 2454-4248
424 – 431

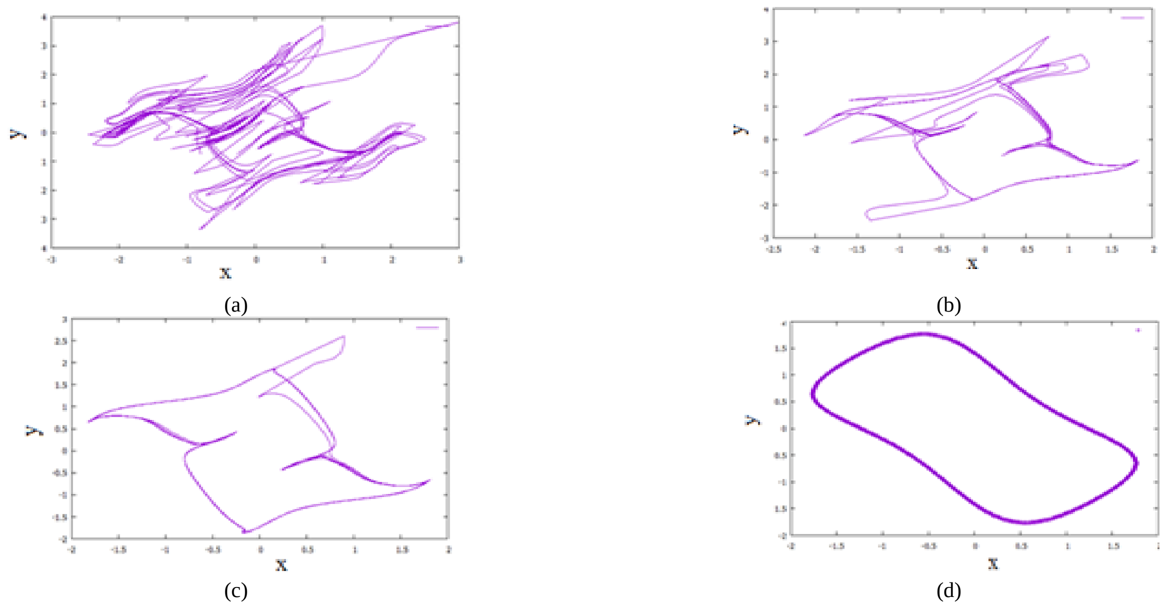

Figure10. Numerically computed phase plane (x-y) plot of RO. system parameters are: α=1.4, β=1.4,b=0.2.(a) a = 1.5, (b) a =1.65 , (c) a =1.78 , (d) a = 2.

In the program, for solving the system equations (9), the value of a has been increased in small steps (0.001) and the steady state output of x is examined for each value of a. The local maxima of oscillating x in time domain have been obtained and plotted along y axis for corresponding a as shown in Fig. 11. Fig. 11 shows variation of x in the range of a from 0.8 to 2.1. From this figure, the nature of generation of oscillation can be observed.

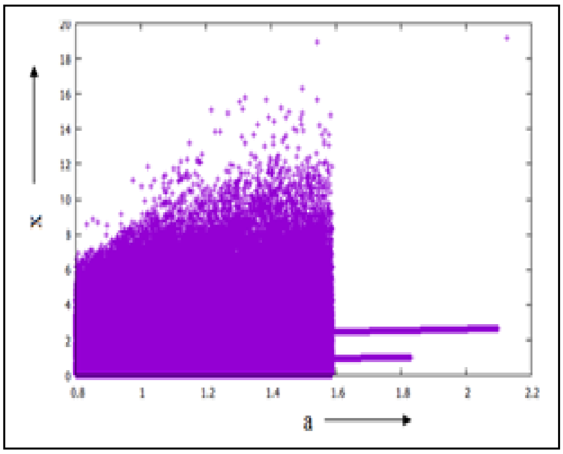

Figure 11. Bifurcation diagram of oscillator output for the range of control parameter a, from a = 0.8 to a = 2.1.

VII. CONCLUSIONS

Detailed studies on the effect of variation of reference voltage on the dynamics of a 3-stage ECL inverter based RO have been done. A hardware experiment has also been performed in the RF band using discrete circuit components. The nature of the RO output is examined in real time as well as in frequency domain. We have also proposed a nonlinear mathematical model for 3-stage RO. For this mathematical modelling of the RO, nonlinear variation of the output voltage with the effective input voltage of individual inverter stage has been considered. Linear stability analysis of the equilibrium points of the oscillator system has been done. It predicts that for a fixed set of system parameters, as the reference voltage control parameter crosses a critical limit, the dynamics of the RO transits from a stable non-oscillatory state to an unstable oscillatory state. Extensive numerical simulation of the system equations has been done. It reveals that the variation of reference voltage results into a number of complex dynamical states of the RO. One would get period doubling scenario leading to chaos in the RO dynamics as a result of the tuning of the dc reference voltage. Experimental observations agree well with the simulation results. The variation of chaotic state with reference voltage has significant implications in the respect of application of chaotic ROs in practical fields. In chaos based secure communications, by varying the reference voltage of the RO, information bits can be mapped into chaotic oscillations of different characters.

REFERENCES

[1] B. Razarvi, Design of analog CMOS integrated Circuits, McGrow Hill, New York, 2001.

[2] S. Z. Lee, B. Kim and K. Lee, "A Novel High Speed Ring Oscillator for Multiphase Clock Generation using Negative Skewed Delay Scheme," IEEE J. Solid State Circuits, vol. 32, Feb 1997, pp. 289-291.

[3] A. Hajimiri, S. Limotyrakis and T. Lee, "Jitter and phase noise in ring oscillators," IEEE J. Solid-State Circuits, vol. 34, 1999, pp. 790–804.

[4] M. Grozing, B. Philipp and M. Berroth, "CMOS ring oscillator with quadrature outputs and 100MHz to 3.5GHz

ISSN: 2454-4248
424 – 431

tuning range," Proc. European Conf. Solid-State Circuits, ESSCIRC 03, IEEE cat. No 03EX 705, Portugal, 2003, pp. 679-682.

[5] Y. Eken and J. Uyemura, "A 5.9GHz voltage-controlled ring oscillator in 0.18 µm CMOS," IEEE J. Solid-State Circuits, vol. 39, 2004, pp. 230–233.

[6] Y. Hosokawa, Y. Nishio and A. Ushida, "Chaotic Circuit Using Two Simple Ring Oscillators Coupled by Diodes," Proc. of NOLTA'99, vol. 1, Nov. 1999 pp. 107-110.

[7] A. S. Elwakil and K. N. Salama, "On the Nonlinear Modeling of Ring oscillators," Journal of Circuits, Systems, and Computers, vol.18, no. 4, 2009, pp. 681–696.

[8] M. P. Kennedy, R. Rovatti, G. Setti, Chaotic electronics in telecommunications, Taylor and Francis, 2000.

[9] L. Elarson , L. S. Tsimring, J. M. Litt, Digital Communications using Chaos and Nonlinear Dynamics, Springer, 2006.

[10] H. Shizen, L. Wei, W. Yutong, Z. Lee, "Design of a Voltage Controlled Ring Oscillator based on MOS capacitance," Proc. International Multi Conference of Engineers and Computer Scientists, Hongkong, Vol. 2, 2009, pp. 1526-1528.

[11] L. Sun and T. A. Kwasniewski, "A 1.25 GHz 0.35µm monolithic COMOS PLL based on a multiphase Ring Oscillator," IEEE journal of Solid State Circuits, vol. 36 no. 6, June 2001, pp. 910-916.

[12] M. K. Mondal and B. C. Sarkar, "Ring Oscillator: Characteristics and Applications,' Indian Journal of pure and applied physics, vol.48, February 2010, pp. 136-145.

[13] J. Millman, Microelectronics: Digital and analog Circuits and Systems, Mc grawhill International Student Edition, 1981.

[14] M. E. Valkenberg, Network Analysis, 3rd edition, Prentice Hall of India, 2007, pp. 307-310.

[15] S. S. Sastry, "Introductory methods of numerical analysis," PHI Learning Pvt. Ltd., 2005.